Journal of Earth and Planetary System Science
Volume 1, Issue 1, 62-74.
e_ISSN:
https://journal.gomit.id/jepss
DOI:

Forecasting Monthly Rainfall Variability in the Indragiri Region, Indonesia, Using Seasonal ARIMA: Dataset Reconstruction, Model Evaluation, and Out-of-Sample Validation

Cahyo Adi Nugroho *
Sekolah Tinggi Meteorologi Klimatologi & Geofisika,
INDONESIA

*** Corresponding author:**
Cahyo Adi Nugroho, Sekolah Tinggi Meteorologi Klimatologi & Geofisika, INDONESIA.
cahyoadinugroho1100@gmail.com

Article Info

Article history:

Received: September 05, 2026
Revised: September 15, 2026
Accepted: September 16, 2026

Keywords:

rainfall
SARIMA
forecasting
Ljung–Box test
reanalysis

Abstract

Background: Monthly rainfall forecasting is important for water-resource management, agricultural planning, and hydrometeorological risk assessment. However, reliable forecasting requires a temporally consistent dataset and appropriate representation of seasonal rainfall variability.
Aims: This study aims to reconstruct and audit a monthly rainfall dataset for the Indragiri region, identify its temporal and seasonal characteristics, evaluate alternative Seasonal Autoregressive Integrated Moving Average (SARIMA) models, and assess their forecasting performance and residual adequacy.
Methods: Monthly rainfall data derived from reanalysis were reconstructed for January 2014-June 2025, resulting in 138 monthly records. Temporal auditing identified June 2025 as incomplete, containing only 20 of the expected 60 timestamps; therefore, 137 complete months through May 2025 were used for model development. Autocorrelation and partial autocorrelation analyses were conducted to identify temporal and seasonal structures. Eight SARIMA candidates were compared using AIC, BIC, RMSE, MAE, sMAPE, and Ljung–Box residual diagnostics.
Results: The rainfall series had a mean of 16.15 mm, standard deviation of 13.19 mm, and maximum of 49.59 mm, with strong annual seasonality. SARIMA(0,0,2)(2,1,0)[12] achieved the lowest test RMSE (10.36 mm), MAE (6.98 mm), and sMAPE (48.17%). However, significant residual autocorrelation remained at lags 6, 12, 18, and 24 ($p < .001$).
Conclusion: The selected SARIMA model provides a useful seasonal forecasting baseline but does not fully capture the dependence structure of monthly rainfall. Forecasts for July 2025–June 2027 indicate persistent seasonal variability, highlighting the need for additional climatic predictors or alternative models to improve forecasting accuracy.

To cite this article: Nugroho.C.A., (2026). Title. *Forecasting Monthly Rainfall Variability in the Indragiri Region, Indonesia, Using Seasonal ARIMA: Dataset Reconstruction, Model Evaluation, and Out-of-Sample Validation, 1*(1), 62-75.

INTRODUCTION

Rainfall is a central component of the hydroclimate system and a key input to agricultural production, water availability, flood risk, and drought management. At monthly scales, rainfall records frequently exhibit persistence, seasonality, and non-Gaussian variability, which makes their direct extrapolation difficult and motivates statistical time-series approaches (Wilks, 2011; Petropoulos et al., 2022). In tropical regions, the repeating annual cycle is particularly important because the timing of wet and dry periods is often more persistent than the magnitude of individual rainfall events. Forecasting models that represent this seasonal dependence can therefore provide useful baseline information for planning and risk assessment (Hyndman & Athanasopoulos, 2021; Brockwell & Davis, 2016).

Indonesia presents a particularly relevant setting for seasonal rainfall analysis because rainfall variability reflects interactions among monsoonal circulation, local land–sea processes, topography, and large scale ocean–atmosphere variability. Aldrian and Susanto (2003) identified several dominant rainfall regimes across Indonesia and showed strong annual and, in some regions, semi-annual variability. Subsequent studies have documented the roles of ENSO and the Indian Ocean Dipole (IOD) in modulating Indonesian rainfall, with the magnitude and spatial structure of the influence varying by season and region (Hidayat & Ando, 2014; Nur'utami & Hidayat, 2016; As-syakur et al., 2014; Kurniadi et al., 2021). Over Sumatra, rainfall also exhibits strong diurnal and land–sea interactions, underscoring the multi-scale character of the hydroclimate (Mori et al., 2004; Qian, 2020).

For a statistical forecasting study, however, model performance depends first on the quality of the temporal series supplied to the model. Reanalysis or gridded data can provide spatially consistent meteorological information, but extracted datasets may contain duplicate timestamps, incomplete final periods, missing values, or multiple grid-cell values requiring aggregation. ERA5, for example, is designed as an hourly global reanalysis with an ensemble-based uncertainty estimate and continuous long-term coverage, but any downstream extraction still requires explicit quality control before time-series modeling (Hersbach et al., 2020). More generally, hydroclimatic series can contain nonstationarity and scaling behavior that should not be ignored when choosing an appropriate stochastic model (Koutsoyiannis, 2006).

Seasonal ARIMA models provide a transparent framework for representing autoregressive dependence, differencing, and recurring seasonal structure. The Box–Jenkins framework remains foundational for identifying, estimating, and diagnosing ARIMA-family models (Box & Jenkins, 1970; Box et al., 2015). Automated model-selection procedures can accelerate the search over candidate structures, but information criteria alone do not guarantee that a model will forecast well out of sample or that its residuals will be independent (Akaike, 1974; Hyndman & Khandakar, 2008; Hyndman & Koehler, 2006). Forecast evaluation therefore benefits from explicit train–test separation and model diagnostics (Tashman, 2000; Bergmeir et al., 2018).

Rainfall presents an additional challenge because near-zero values and high-rainfall episodes generate asymmetric and heavy-tailed behavior. Consequently, conventional percentage errors can become unstable, and residual normality should not be treated as the only criterion for a useful forecasting model. Forecast accuracy should instead be assessed with complementary scale-dependent measures such as MAE and RMSE, while residual dependence should be examined explicitly (Hyndman & Koehler, 2006; Gneiting & Katzfuss, 2014). The Ljung–Box test is widely used to determine whether the residual autocorrelations as a group are consistent with white noise (Ljung & Box, 1978).

Against this background, this study focuses on the Indragiri region of Riau and addresses a practical but often overlooked problem: how to obtain a defensible monthly rainfall forecasting series from reanalysis-derived data and evaluate a seasonal model beyond AIC alone. The contribution is therefore methodological rather than a claim that SARIMA is universally optimal. The workflow explicitly documents data reconstruction and completeness checks, identifies annual dependence through ACF and PACF, compares multiple SARIMA specifications using a held-out test period, and evaluates residual independence before producing a 24-month forecast. This design follows the broader forecasting literature emphasizing reproducibility, out-of-sample evaluation, probabilistic uncertainty, and transparent diagnostics (Armstrong, 2001; Diebold & Mariano, 1995; Makridakis & Hibon, 2000; Makridakis et al., 2020; Petropoulos et al., 2022).

METHOD

2.1 Data Source and Study Series

The analysis uses four reanalysis-derived GRIB files containing rainfall and temperature variables. The study treats rainfall as the primary dependent variable and retains temperature as ancillary information for future extension to a dynamic-regression or SARIMAX formulation. The present paper does not use temperature as an exogenous predictor, so the fitted model is substantively a SARIMA model rather than a regression-with-exogenous-input SARIMAX model.

2.2 Data Reconstruction and Quality Control

The raw extraction contained multiple spatial values at each timestamp. The reconstruction procedure first aggregated the spatial values at each timestamp and then accumulated the rainfall values into calendar months. The resulting monthly file contained 138 records from January 2014 through June 2025. Quality control checked for duplicate monthly periods, missing months, missing values in the principal rainfall field, negative rainfall totals, and incomplete temporal coverage. A full month in the source series is represented by two timestamps per day; thus, the expected monthly count varies with month length. A month was flagged as partial when its timestamp count was below 90% of the modal monthly count.

Table 1. Monthly rainfall data quality-control summary.

Quality-control item	Result
Total monthly records	138
Date range	January 2014–June 2025
Duplicate months	0
Missing months	0
Monthly rainfall missing values	0
Negative rainfall values	0
Complete months used in modeling	137
Partial month	June 2025 (20 of 60 expected timestamps)

The audit shows that June 2025 is not a complete monthly observation. The reconstructed file records 3.490 mm for that month but only 20 timestamps, versus 60 timestamps expected for a complete 30-day month. The principal modeling series therefore ends in May 2025, retaining 137 complete monthly observations. The original monthly file and audit fields document these conditions explicitly.

2.3 Exploratory Analysis

The rainfall series was summarized using the mean, standard deviation, quartiles, minimum, and maximum. Temporal dependence was examined using the sample autocorrelation function (ACF) and partial autocorrelation function (PACF) up to lag 36. Because a 12-month cycle is the natural seasonal period for monthly rainfall, particular attention was given to lags 12, 24, and 36. ACF/PACF interpretation followed the standard Box–Jenkins identification framework (Box & Jenkins, 1970; Box et al., 2015; Hamilton, 1994; Shumway & Stoffer, 2017).

2.4 SARIMA Model

The seasonal autoregressive integrated moving average model is denoted SARIMA(p,d,q)(P,D,Q)s, where p, d, and q represent the non-seasonal autoregressive, differencing, and moving-average orders, respectively; P, D, and Q denote their seasonal counterparts; and s is the seasonal period. The general multiplicative model can be written as:

$$(1-\varphi_1 B-\cdots-\varphi_{\mathrm{p}} B^{\mathrm{p}})(1-\Phi_1 B^{\mathrm{s}}-\cdots-\Phi_{\mathrm{p}} B^{\mathrm{Ps}})(1-B)^{\mathrm{d}}(1-B^{\mathrm{s}})$$
$$=(1+\theta_1 B+\cdots+\theta q B q)(1+\Theta_1 B^{\mathrm{s}}+\cdots+\Theta Q B Q^{\mathrm{s}})\varepsilon_{\mathrm{t}}.$$

Candidate structures were selected from the observed seasonal dependence and from automated stepwise search, then compared using AIC/BIC and out-of-sample performance. Information criteria reward good fit while penalizing model complexity (Akaike, 1974; Schwarz, 1978). In forecasting applications, however, a lower information criterion is not sufficient if the model fails to deliver acceptable prediction accuracy or leaves strong dependence in its residuals (Hyndman & Athanasopoulos, 2021; Makridakis & Hibon, 2000).

2.5 Train–Test Design and Accuracy Measures

To avoid evaluating a model on observations used for estimation, the last 12 complete months were reserved for testing. The training period therefore spans January 2014–May 2024 (125 months), and the testing period spans June 2024–May 2025 (12 months). This fixed-origin holdout design follows standard out-of-sample forecasting practice and avoids the leakage concerns associated with inappropriate random cross-validation for dependent data (Tashman, 2000; Bergmeir et al., 2018).

Forecast accuracy was assessed using RMSE, MAE, and sMAPE. RMSE is defined as sqrt[(1/n) $\Sigma(y_t - \hat{y}_t)^2$], whereas MAE is (1/n) $\Sigma|y_t - \hat{y}_t|$. sMAPE was used as an additional descriptive measure, but it was not treated as the principal criterion because very small rainfall denominators can make percentage-based errors unstable (Hyndman & Koehler, 2006).

2.6 Residual Diagnostics

For an adequate stochastic forecasting model, residuals should contain little or no systematic temporal information. Residual diagnostics therefore considered the residual time plot, histogram, Q–Q plot, ACF, PACF, Jarque–Bera normality test, and the Ljung–Box portmanteau test. The Ljung–Box statistic tests the joint null hypothesis that autocorrelations up to a specified lag are zero; a small p-value indicates remaining serial dependence (Ljung & Box, 1978). Residual autocorrelation and squared-residual dependence can also signal model misspecification or nonlinear variance structure (Box & Pierce, 1970; McLeod & Li, 1983).

2.7 Software and Reproducibility

The analytical workflow was implemented in Python using pandas for tabular data handling and statsmodels for time-series estimation and diagnostics. The methodological choices are consistent with established work on decomposition and exponential smoothing (Cleveland et al., 1990; Gardner, 1985, 2006; Hyndman et al., 2002), probabilistic and competitive forecasting (Gneiting & Katzfuss, 2014; Gneiting & Raftery, 2007; Makridakis & Hibon, 2000; Makridakis et al., 2020), time-series theory and state-space representation (Hamilton, 1994; Harvey, 1989 ; Shumway & Stoffer, 2017), and residual dependence testing (Box & Pierce, 1970; Ljung & Box, 1978; McLeod & Li, 1983). These references support the use of information criteria, predictive accuracy, and residual diagnostics as complementary criteria rather than interchangeable measures. Software documentation follows the pandas and statsmodels literature (McKinney, 2010; Seabold & Perktold, 2010).

RESULTS AND DISCUSSION

3.1 Rainfall Characteristics

After removal of the incomplete June 2025 record, the modeling series contains 137 complete monthly observations from January 2014 to May 2025. The rainfall mean is 16.15 mm and the standard deviation is 13.19 mm. The median is 16.09 mm, while the minimum and maximum are 0.026 mm and 49.59 mm, respectively. The distribution is therefore broad, with repeated very low rainfall months and several months close to 40–50 mm. The monthly audit file confirms 137 observations for the modeling period and no negative rainfall values.

Table 2. Descriptive statistics of the complete monthly rainfall series.

Statistic	Value
N	137
Mean (mm)	16.150
Standard deviation (mm)	13.194
Minimum (mm)	0.026
25th percentile (mm)	2.237
Median (mm)	16.092
75th percentile (mm)	28.870
Maximum (mm)	49.589

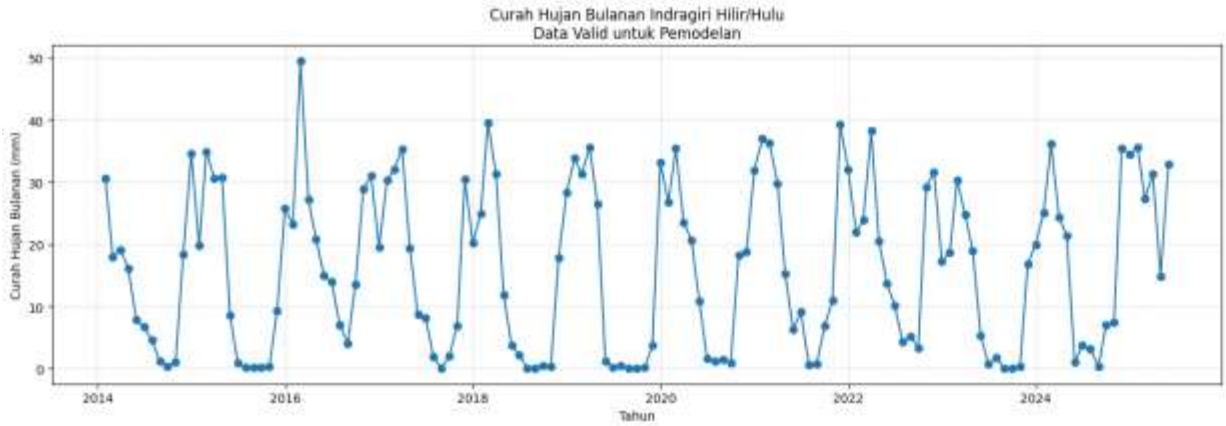

Figure 1. Monthly rainfall series used for the principal SARIMA analysis (January 2014–May 2025).

The time series exhibits a repeating annual pattern, with prolonged low-rainfall periods and recurrent increases toward wetter months. Similar annual and semi-annual variability has been documented across Indonesian rainfall regimes, although the precise timing and intensity vary geographically (Aldrian & Susanto, 2003; Hidayat & Ando, 2014). The visible seasonality also agrees with studies linking Indonesian rainfall variability to Indo-Pacific climate drivers and regional circulation (Nur'utami & Hidayat, 2016; Kurniadi et al., 2021; Qian, 2020).

3.2 Autocorrelation Structure

The ACF of monthly rainfall shows substantial short-lag dependence and pronounced oscillation across successive years, with notable structure around the annual cycle. The PACF likewise shows a strong first-lag component and several early-lag effects before tapering. These features support the inclusion of a 12-month seasonal period and motivate seasonal differencing in a subset of candidate models. The observed pattern is consistent with a time series in which the month-to-month state and the corresponding season in preceding years both contribute information for forecasting (Box & Jenkins, 1970; Hyndman & Athanasopoulos, 2021; Shumway & Stoffer, 2017).

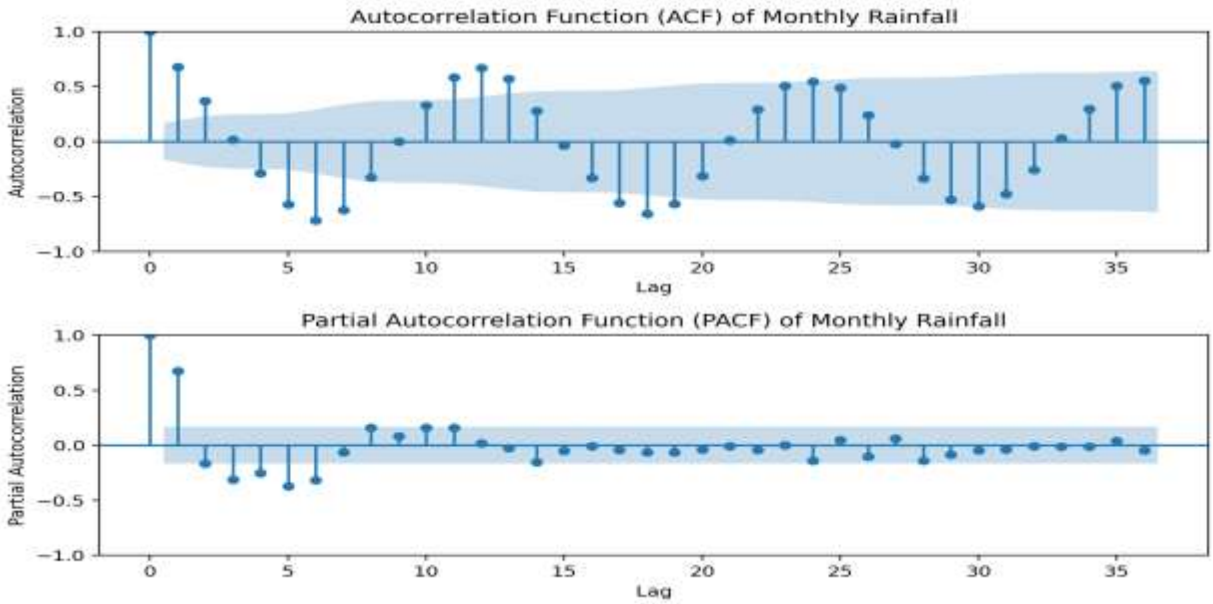

Figure 2. Autocorrelation and partial autocorrelation of the monthly rainfall series.

3.3 Candidate SARIMA Model Comparison

Eight SARIMA candidates with a seasonal period of 12 months were fitted to the 125-month training sample. The comparison indicates that the lowest test RMSE was obtained by SARIMA(0,0,2)(2,1,0)[12], with RMSE = 10.3560 mm and MAE = 6.9761 mm. The model had an AIC of 621.583 and BIC of 636.515 on the training set. Several alternatives had lower AIC values but slightly worse test RMSE, illustrating why model selection should combine fit criteria and out-of-sample forecasting performance rather than use AIC alone.

Table 3. Out-of-sample performance of candidate SARIMA models on June 2024–May 2025.

Model	AIC	RMSE (mm)	MAE (mm)	sMAPE (%)
SARIMA(2,0,0)(2,1,0)[12]	608.543	10.591	7.219	51.917
SARIMA(2,0,1)(2,1,0)[12]	609.320	10.547	7.166	63.730
SARIMA(1,0,0)(2,1,0)[12]	613.217	10.474	7.080	48.917
SARIMA(1,0,1)(2,1,0)[12]	614.970	10.455	7.060	48.288
SARIMA(0,0,1)(2,1,0)[12]	619.644	10.358	6.985	49.046
SARIMA(0,0,0)(2,1,0)[12]	619.959	10.428	6.992	46.754
SARIMA(0,0,2)(2,1,0)[12]	621.583	10.356	6.976	48.168
SARIMA(1,0,0)(1,1,0)[12]	721.981	11.783	8.646	65.802

The lowest RMSE belongs to SARIMA(0,0,2)(2,1,0)[12], but the practical difference from SARIMA(0,0,1)(2,1,0)[12] is small. More importantly, all eight models fail the residual white-noise requirement used in this study. Thus, the selected specification is the best predictive candidate among the tested models, not an unequivocally adequate error-generating model. This distinction is important in forecasting because correlated residuals imply that some information remains unmodeled (Hyndman & Athanasopoulos, 2021).

3.4 Residual Diagnostics

The diagnostic results for the selected SARIMA(0,0,2)(2,1,0)[12] model are mixed. The residual time series oscillates around a variable center and contains several relatively large positive and negative values. The residual distribution is right-skewed and departs visibly from the theoretical normal line. The Jarque–Bera statistic is 23.897 with $p = 0.000006$, indicating significant non-normality. However, non-normality alone does not determine forecasting usefulness; residual independence is the more direct diagnostic for whether systematic temporal information remains in the errors (Hyndman & Athanasopoulos, 2021; Gneiting & Katzfuss, 2014).

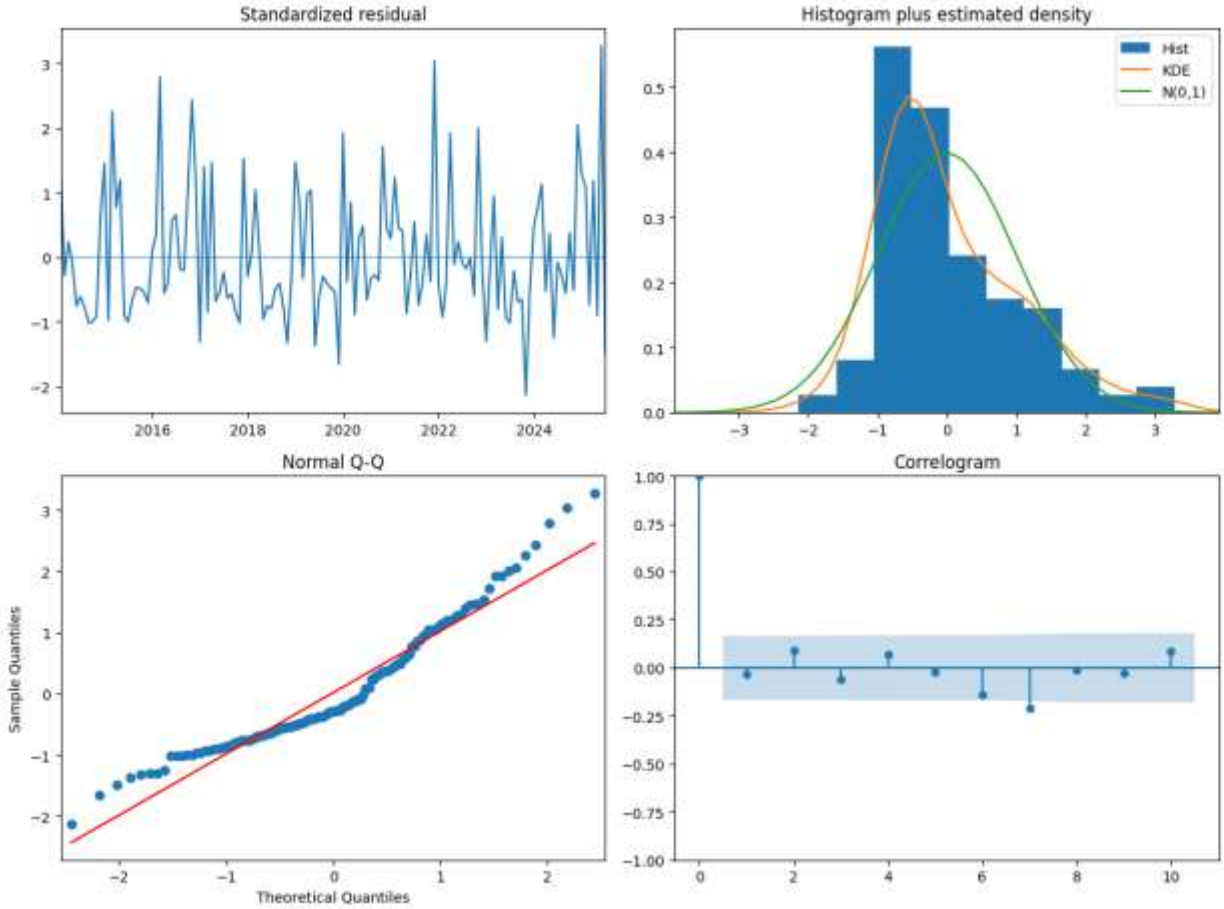

Figure 3. Residual diagnostics for the selected SARIMA(0,0,2)(2,1,0)[12] candidate, including standardized residuals, distribution, Q–Q plot, and correlogram.

The key limitation is the Ljung–Box result. At lags 6, 12, 18, and 24, p-values are all below 0.001, so the null hypothesis of no joint autocorrelation is rejected. This indicates that the selected model leaves statistically significant temporal structure in the residuals. The finding is consistent with the residual ACF/PACF images, which show several departures from the confidence bands. In the forecasting literature, such residual dependence is a warning that the current model has not exhausted the predictable structure of the series (Ljung & Box, 1978; Box & Pierce, 1970; Hyndman & Athanasopoulos, 2021).

Table 4. Ljung–Box diagnostic for the selected candidate model.

Lag	Ljung–Box Q	p-value
6	31.683	0.000019
12	43.113	0.000022
18	47.103	0.000204
24	53.832	0.000449

Because every candidate failed the white-noise criterion, the study does not interpret the residual diagnostic failure as evidence that rainfall forecasting is impossible. Rather, it shows that the eight tested low-order specifications are insufficient to represent all serial dependence in this particular dataset. This is compatible with forecasting case studies where no single candidate satisfies every diagnostic simultaneously, particularly when the series contains strong seasonal structure and irregular extremes (Hyndman & Athanasopoulos, 2021).

3.5 Validation Against the Held-Out Period

The held-out validation period is June 2024–May 2025. The selected candidate predicts the broad seasonal shape but systematically underestimates several high-rainfall months. The largest miss occurs in May 2025, when the observed rainfall is 32.835 mm while the model predicts only 4.884 mm, an absolute error of 27.951 mm. The model also underpredicts November 2024, December 2024, and January 2025. These errors demonstrate that seasonal persistence alone is insufficient to reproduce every high-rainfall episode.

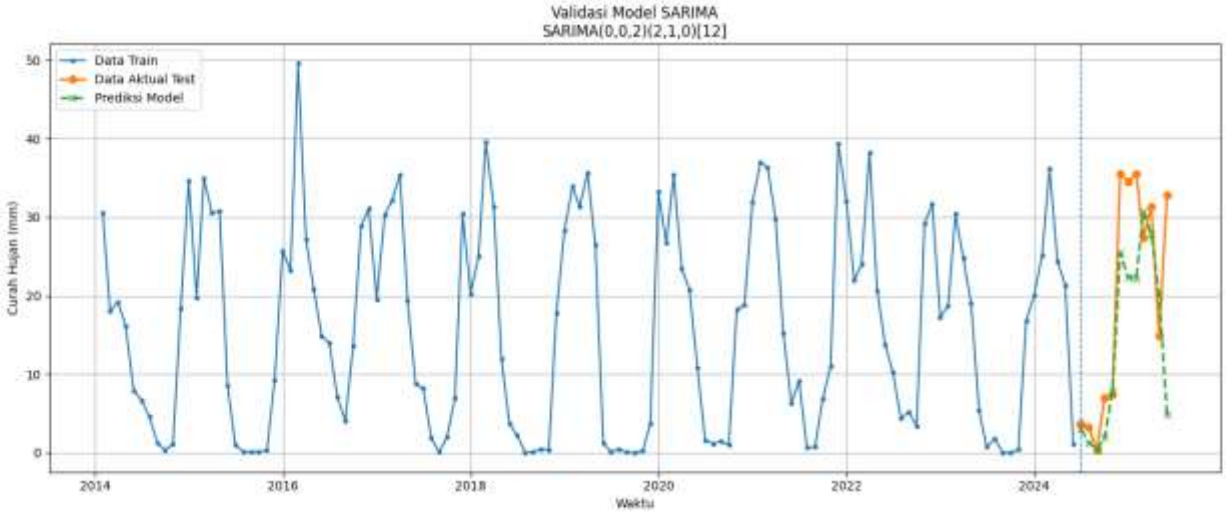

Figure 4. Out-of-sample validation of the selected SARIMA model for June 2024–May 2025.

3.6 Final Forecast: July 2025–June 2027

After candidate comparison, the selected model SARIMA(0,0,2)(2,1,0)[12] was re-estimated using all 137 complete months, January 2014–May 2025. The final full-sample fit has AIC = 712.903 and BIC = 728.594. Because June 2025 was excluded as a partial observation, the 24-month forecasting horizon begins in July 2025. Forecasts display a persistent annual cycle, with low values in the middle of the year and higher values toward the end of the year and early wet season.

Table 5. Monthly rainfall forecast for July 2025–June 2027 from the full-sample selected model.

Period	Forecast (mm)	Lower 95% (mm)	Upper 95% (mm)
2025-07	10.004	0.000	25.240
2025-08	3.844	0.000	19.267
2025-09	2.158	0.000	17.583
2025-10	4.598	0.000	20.023
2025-11	15.094	0.000	30.520
2025-12	31.418	15.993	46.844
2026-01	25.677	10.252	41.103
2026-02	27.424	11.998	42.849
2026-03	29.683	14.258	45.109
2026-04	27.758	12.333	43.184
2026-05	17.326	1.901	32.752
2026-06	17.642	2.216	33.067
2026-07	5.425	0.000	22.428
2026-08	2.874	0.000	19.915
2026-09	1.011	0.000	18.051
2026-10	3.054	0.000	20.095
2026-11	8.191	0.000	25.232
2026-12	26.096	9.055	43.136
2027-01	24.559	7.518	41.600
2027-02	27.536	10.495	44.576
2027-03	31.891	14.850	48.932
2027-04	26.848	9.807	43.889
2027-05	18.534	1.493	35.575

2027-06	13.046	0.000	30.087

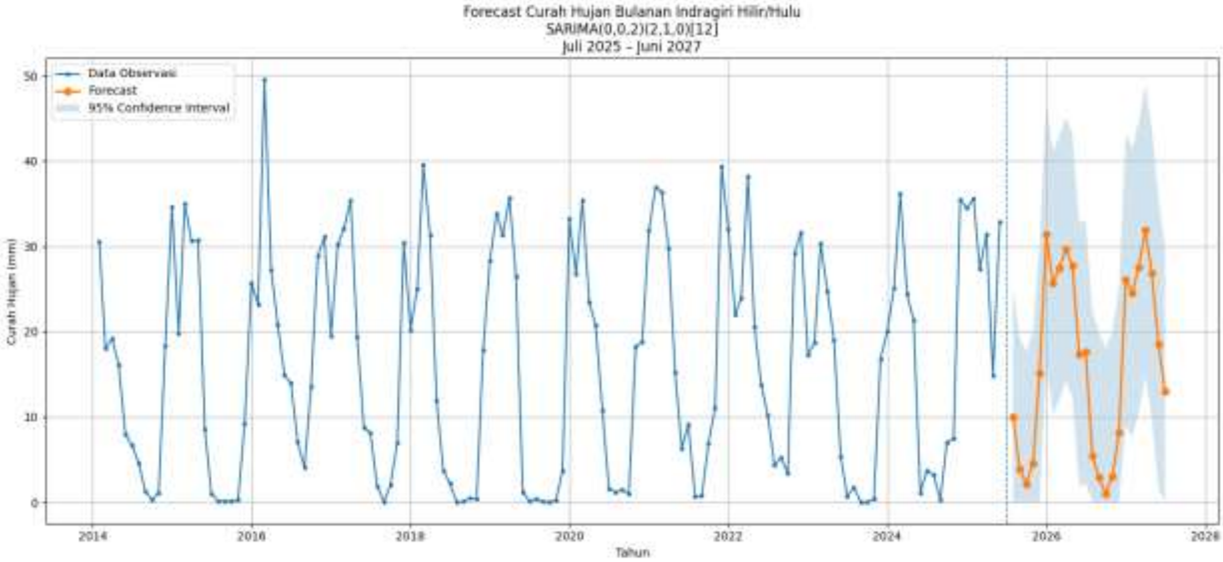

Figure 5. Twenty-four-month rainfall forecast with 95% confidence intervals.

The 24-month forecast has a mean of 16.737 mm. The highest predicted value is 31.891 mm in March 2027, while the lowest is 1.011 mm in September 2026. The confidence intervals widen for longer horizons, reflecting increasing forecast uncertainty. Negative lower bounds produced by the Gaussian state-space prediction distribution were clipped at zero for presentation because rainfall cannot be negative; the clipping is a physical-display constraint and does not alter the fitted model or point forecast. Probabilistic forecasting frameworks emphasize the need to distinguish point forecasts from the full predictive distribution and its uncertainty (Gneiting & Katzfuss, 2014; Gneiting & Raftery, 2007).

CONCLUSION

This study established a reproducible workflow for converting reanalysis-derived rainfall data into a validated monthly series for the Indragiri region and for evaluating seasonal ARIMA models using both predictive and diagnostic criteria. The initial dataset contained 138 monthly records from January 2014 to June 2025. Quality control identified June 2025 as temporally incomplete, reducing the principal modeling sample to 137 complete months from January 2014 to May 2025. The rainfall series exhibits strong annual seasonality and substantial temporal persistence, supporting a seasonal period of 12 months.

Among eight candidate SARIMA models, SARIMA(0,0,2)(2,1,0)[12] achieved the lowest out-of-sample RMSE (10.356 mm) and MAE (6.976 mm). Nevertheless, the model failed the residual white-noise criterion, with Ljung–Box p-values below 0.001 at lags 6, 12, 18, and 24. The model should therefore be interpreted as a useful seasonal baseline rather than as a fully adequate stochastic representation of the rainfall process. Its principal strength is the reproduction of the dominant annual cycle; its principal weakness is the persistence of residual dependence and the underestimation of selected high-rainfall episodes.

When refitted to all 137 complete months, the selected model produced a 24-month forecast for July 2025–June 2027 with an average of 16.737 mm. The forecast peaks at 31.891 mm in March 2027 and reaches a minimum of 1.011 mm in September 2026. Future work should extend the baseline by testing richer seasonal structures, transformation-based models, benchmark methods, and dynamic regression with large-scale climate predictors. Independent validation against station observations should also be undertaken before the forecast is used for operational decision-making.

ACKNOWLEDGMENT

The author would like to express his gratitude to the Sekolah Tinggi Meteorologi Klimatologi dan Geofisika (STMKG) for providing the academic environment and necessary facilities that supported the completion of this research. This research received no specific grant from any funding agency in the public, commercial, or not-for-profit sectors.

AUTHOR CONTRIBUTION STATEMENT

Cahyo Adi Nugroho conceptualized the core research idea, designed the methodology, developed the time-series modeling framework, conducted the data analysis, and wrote the original manuscript and final version.

AI DISCLOSURE STATEMENT

The author used the Gemini large language model and Claude AI during the preparation of this work for refining sentence structures, translating content into academic English, expanding the theoretical framework, and improving the overall readability of the manuscript. After using these tools, the author thoroughly reviewed and edited the content as needed and takes full responsibility for the content of the publication.

CONFLICTS OF INTEREST

The author declares no conflict of interest. This research was conducted purely for academic purposes. The author confirms the absence of any potential conflicts of interest—financial, institutional, or personal—that could influence the conduct of this study, the analysis of data, the preparation of the manuscript, or its publication.

REFERENCES

Akaike, H. (1974). A new look at the statistical model identification. IEEE Transactions on Automatic Control, 19(6), 716–723. https://doi.org/10.1109/TAC.1974.1100705

Armstrong, J. S. (Ed.). (2001). Principles of forecasting: A handbook for researchers and practitioners. Springer. https://doi.org/10.1007/978-0-306-47630-3

As-syakur, A. R., Adnyana, I. W. S., Mahendra, M. S., Arthana, I. W., Kasa, I. W., Ekayanti, N. W., Nuarsa, I. W., & Sunarta, I. N. (2014). Observation of spatial patterns on the rainfall response to ENSO and IOD over Indonesia using TRMM Multisatellite Precipitation Analysis (TMPA). International Journal of Climatology, 34(15), 3880–3893. https://doi.org/10.1002/joc.3939

Bergmeir, C., Hyndman, R. J., & Koo, B. (2018). A note on the validity of cross-validation for evaluating autoregressive time series prediction. Computational Statistics & Data Analysis, 120, 70–83. https://doi.org/10.1016/j.csda.2017.11.003

Box, G. E. P., & Jenkins, G. M. (1970). Time series analysis: Forecasting and control. Holden-Day.

Box, G. E. P., & Pierce, D. A. (1970). Distribution of residual autocorrelations in autoregressive-integrated moving average time series models. Journal of the American Statistical Association, 65(332), 1509–1526. https://doi.org/10.1080/01621459.1970.10481180

Box, G. E. P., Jenkins, G. M., Reinsel, G. C., & Ljung, G. M. (2015). Time series analysis: Forecasting and control (5th ed.). Wiley.

Bridhikitti, A. (2013). Connections of ENSO/IOD and aerosols with Thai rainfall anomalies and associated implications for local rainfall forecasts. International Journal of Climatology, 33(13), 2836–2845. https://doi.org/10.1002/joc.3630

Brockwell, P. J., & Davis, R. A. (2016). Introduction to time series and forecasting (3rd ed.). Springer. https://doi.org/10.1007/978-3-319-29854-2

Chatfield, C. (2000). Time-series forecasting. Chapman & Hall/CRC.

Cleveland, R. B., Cleveland, W. S., McRae, J. E., & Terpenning, I. (1990). STL: A seasonal-trend decomposition procedure based on loess. Journal of Official Statistics, 6(1), 3–73.

Dickey, D. A., & Fuller, W. A. (1979). Distribution of the estimators for autoregressive time series with a unit root. Journal of the American Statistical Association, 74(366a), 427–431. https://doi.org/10.1080/01621459.1979.10482531

Diebold, F. X., & Mariano, R. S. (1995). Comparing predictive accuracy. Journal of Business & Economic Statistics, 13(3), 253–263. https://doi.org/10.1080/07350015.1995.10524599

Gardner, E. S. (1985). Exponential smoothing: The state of the art. Journal of Forecasting, 4(1), 1–28. https://doi.org/10.1002/for.3980040103

Gardner, E. S. (2006). Exponential smoothing: The state of the art—Part II. International Journal of Forecasting, 22(4), 637–666. https://doi.org/10.1016/j.ijforecast.2006.03.003

Gneiting, T., & Katzfuss, M. (2014). Probabilistic forecasting. Annual Review of Statistics and Its Application, 1, 125–151. https://doi.org/10.1146/annurev-statistics-062713-085831

Gneiting, T., & Raftery, A. E. (2007). Strictly proper scoring rules, prediction, and estimation. Journal of the American Statistical Association, 102(477), 359–378. https://doi.org/10.1198/016214506000001437

Gobin, A., Nguyen, H. T., Pham, V. Q., & Pham, H. T. T. (2016). Heavy rainfall patterns in Vietnam and their relation with ENSO cycles. International Journal of Climatology, 36(4), 1686–1699. https://doi.org/10.1002/joc.4451

Hamilton, J. D. (1994). Time series analysis. Princeton University Press.

Harvey, A. C. (1989). Forecasting, structural time series models and the Kalman filter. Cambridge University Press.

Haylock, M. R., Peterson, T. C., Alves, L. M., Ambrizzi, T., Anunciação, Y. M. T., Baez, J., Barros, V. R., Berlato, M. A., Bidegain, M., Coronel, G., Corradi, V., Garcia, V. J., Grimm, A. M., Karoly, D., Marengo, J. A., Marino, M. B., Moncunill, D. F., Nechet, D., Quintana, J., … Vincent, L. A. (2006). Trends in total and extreme South American rainfall in 1960–2000 and links with sea surface temperature. Journal of Climate, 19(8), 1490–1512. https://doi.org/10.1175/JCLI3695.1

Hersbach, H., Bell, B., Berrisford, P., Hirahara, S., Horányi, A., Muñoz-Sabater, J., Nicolas, J., Peubey, C., Radu, R., Schepers, D., Simmons, A., Soci, C., Abdalla, S., Abellan, X., Balsamo, G., Bechtold, P., Biavati, G., Bidlot, J., Bonavita, M., … Thépaut, J.-N. (2020). The ERA5 global reanalysis.

Quarterly Journal of the Royal Meteorological Society, 146(730), 1999–2049. https://doi.org/10.1002/qj.3803
Hidayat, R., & Ando, K. (2014). Variabilitas curah hujan Indonesia dan hubungannya dengan ENSO/IOD: Estimasi menggunakan data JRA-25/JCDAS. Agromet, 28(1), 1–8. https://doi.org/10.29244/j.agromet.28.1.1-8
Hurst, H. E. (1951). Long-term storage capacity of reservoirs. Transactions of the American Society of Civil Engineers, 116(1), 770–799. https://doi.org/10.1061/TACEAT.0006518
Hyndman, R. J., & Athanasopoulos, G. (2021). Forecasting: Principles and practice (3rd ed.). OTexts. https://otexts.com/fpp3/
Hyndman, R. J., & Khandakar, Y. (2008). Automatic time series forecasting: The forecast package for R. Journal of Statistical Software, 27(3), 1–22. https://doi.org/10.18637/jss.v027.i03
Hyndman, R. J., & Koehler, A. B. (2006). Another look at measures of forecast accuracy. International Journal of Forecasting, 22(4), 679–688. https://doi.org/10.1016/j.ijforecast.2006.03.001
Hyndman, R. J., Koehler, A. B., Snyder, R. D., & Grose, S. (2002). A state space framework for automatic forecasting using exponential smoothing methods. International Journal of Forecasting, 18(3), 439–454. https://doi.org/10.1016/S0169-2070(01)00110-8
Jolliffe, I. T. (2002). Principal component analysis (2nd ed.). Springer. https://doi.org/10.1007/b98835
Koutsoyiannis, D. (2006). Nonstationarity versus scaling in hydrology. Journal of Hydrology, 324(1–4), 239–254. https://doi.org/10.1016/j.jhydrol.2005.09.022
Kurniadi, A., Weller, E., Min, S.-K., & Seong, M.-G. (2021). Independent ENSO and IOD impacts on rainfall extremes over Indonesia. International Journal of Climatology, 41(6), 3640–3656. https://doi.org/10.1002/joc.7040
Kwiatkowski, D., Phillips, P. C. B., Schmidt, P., & Shin, Y. (1992). Testing the null hypothesis of stationarity against the alternative of a unit root. Journal of Econometrics, 54(1–3), 159–178. https://doi.org/10.1016/0304-4076(92)90104-Y
Leong, M., Juneng, L., Tangang, F., & Salimun, E. (2024). Expansion of winter ENSO-associated rainfall affected area in Southeast Asia under warmer climate. International Journal of Climatology, 44(3), 831–851. https://doi.org/10.1002/joc.8358
Ljung, G. M., & Box, G. E. P. (1978). On a measure of lack of fit in time series models. Biometrika, 65(2), 297–303. https://doi.org/10.1093/biomet/65.2.297
Makridakis, S., & Hibon, M. (2000). The M3-Competition: Results, conclusions and implications. International Journal of Forecasting, 16(4), 451–476. https://doi.org/10.1016/S0169-2070(00)00057-1
Makridakis, S., Spiliotis, E., & Assimakopoulos, V. (2020). The M4 Competition: 100,000 time series and 61 forecasting methods. International Journal of Forecasting, 36(1), 54–74. https://doi.org/10.1016/j.ijforecast.2019.04.014
Mann, H. B. (1945). Nonparametric tests against trend. Econometrica, 13(3), 245–259. https://doi.org/10.2307/1907187
Maraun, D. (2016). Bias correcting climate change simulations—A critical review. Current Climate Change Reports, 2, 211–220. https://doi.org/10.1007/s40641-016-0050-x
McKinney, W. (2010). Data structures for statistical computing in Python. In S. van der Walt & J. Millman (Eds.), Proceedings of the 9th Python in Science Conference (pp. 51–56).
McLeod, A. I., & Li, W. K. (1983). Diagnostic checking ARMA time series models using squared-residual autocorrelations. Journal of Time Series Analysis, 4(4), 269–273. https://doi.org/10.1111/j.1467-9892.1983.tb00373.x
Mori, S., Hamada, J.-I., Tauhid, Y. I., Yamanaka, M. D., Okamoto, N., Murata, F., Sakurai, N., Hashiguchi, H., & Sribimawati, T. (2004). Diurnal land–sea rainfall peak migration over Sumatera Island, Indonesian Maritime Continent, observed by TRMM satellite and intensive rawinsonde soundings. Monthly Weather Review, 132(8), 2021–2039. https://doi.org/10.1175/1520-0493(2004)132<2021:DLRPMO>2.0.CO;2
Nur'utami, M. N., & Hidayat, R. (2016). Influences of IOD and ENSO to Indonesian rainfall variability: Role of atmosphere-ocean interaction in the Indo-Pacific sector. Procedia Environmental Sciences, 33, 196–203. https://doi.org/10.1016/j.proenv.2016.03.070
Partal, T., & Kahya, E. (2006). Trend analysis in Turkish precipitation data. Hydrological Processes, 20(9), 2011–2026. https://doi.org/10.1002/hyp.5993

Petropoulos, F., Apiletti, D., Assimakopoulos, V., Babai, M. Z., Barrow, D. K., Ben Taieb, S., Bergmeir, C., Bessa, R. J., Bijak, J., Boylan, J. E., Browell, J., Carnevale, C., Castle, J. L., Cirillo, P., Clements, M. P., Cordeiro, C., Cyrino Oliveira, F. L., De Baets, S., Dokumentov, A., … Ziel, F. (2022). Forecasting: Theory and practice. International Journal of Forecasting, 38(3), 705–871. https://doi.org/10.1016/j.ijforecast.2021.11.001

Qian, J.-H. (2020). Multi-scale climate processes and rainfall variability in Sumatra and Malay Peninsula associated with ENSO in boreal fall and winter. International Journal of Climatology. https://doi.org/10.1002/joc.6450

Schwarz, G. (1978). Estimating the dimension of a model. The Annals of Statistics, 6(2), 461–464. https://doi.org/10.1214/aos/1176344136

Seabold, S., & Perktold, J. (2010). statsmodels: Econometric and statistical modeling with Python. In S. van der Walt & J. Millman (Eds.), Proceedings of the 9th Python in Science Conference.

Sen, P. K. (1968). Estimates of the regression coefficient based on Kendall's tau. Journal of the American Statistical Association, 63(324), 1379–1389. https://doi.org/10.1080/01621459.1968.10480934

Shumway, R. H., & Stoffer, D. S. (2017). Time series analysis and its applications: With R examples (4th ed.). Springer. https://doi.org/10.1007/978-3-319-52452-8

Stagge, J. H., Tallaksen, L. M., Gudmundsson, L., Van Loon, A. F., & Stahl, K. (2015). Candidate distributions for climatological drought indices (SPI and SPEI). International Journal of Climatology, 35(13), 4027–4040. https://doi.org/10.1002/joc.4267

Tashman, L. J. (2000). Out-of-sample tests of forecasting accuracy: An analysis and review. International Journal of Forecasting, 16(4), 437–450. https://doi.org/10.1016/S0169-2070(00)00065-0

Vicente-Serrano, S. M., Beguería, S., & López-Moreno, J. I. (2010). A multiscalar drought index sensitive to global warming: The standardized precipitation evapotranspiration index. Journal of Climate, 23(7), 1696–1718. https://doi.org/10.1175/2009JCLI2909.1

Wilks, D. S. (2011). Statistical methods in the atmospheric sciences (3rd ed.). Academic Press.

World Meteorological Organization. (2012). Standardized precipitation index user guide (WMO-No. 1090). WMO.

Zhou, Z., Ren, J., He, X., & Liu, S. (2021). A comparative study of extensive machine learning models for predicting long-term monthly rainfall with an ensemble of climatic and meteorological predictors. Hydrological Processes, 35(11), e14424. https://doi.org/10.1002/hyp.14424